Intersubband transitions in InAs/GaSb semimetallic superlattices

A. J. L. Poulter, M. Lakrimi, R. J. Nicholas, N. J. Mason, and P. J. Walker
Clarendon Laboratory, Department of Physics, University of Oxford, Parks Road, Oxford, OX1 3PU, United Kingdom
(Received 24 August 1998)

We report parallel magnetic-field-activated intersubband absorption in InAs/GaSb semimetallic superlattices. The samples were studied in the Voigt configuration enabling normal-incidence excitation of the intersubband transition. For samples with narrow wells, the small absorption coefficient meant that an alternative waveguide configuration was used, again with magnetic field applied parallel to the superlattice layers. In this latter configuration we see further activation of the intersubband resonance by the parallel field as well as new transitions to higher subbands. The intersubband energy and absorption characteristics are studied over a large range of well widths and compared with results from eight-band $\mathbf{k}\cdot\mathbf{p}$ calculations. [S0163-1829(99)03416-5]

I. INTRODUCTION

Intersubband transitions in quantum-well structures are extremely important in making devices to operate in the mid to far infrared (4–20 μm) region of the spectrum,[1] with many commercial applications, especially in the environmental and medical sectors,[2,3] requiring sources and detectors. The recent use of intersubband transitions as the active part of the quantum cascade laser, operating in the region from 11 to 17 μm, has confirmed their importance.[4,5] One of the most promising material systems for infrared applications is InAs/GaSb.[6,7,8] InAs/GaSb heterostructures are unusual in that they form an extreme type-II system, where the InAs conduction band lies about 150 meV in energy below the GaSb valance band.[9] Superlattices in this system have a semiconducting to semimetallic crossover depending on the extent of the heterostructure confinement of the carriers. In this paper we focus on semimetallic superlattices (period >150 Å), where the GaSb valence-band edge lies above the InAs conduction band and a negative band gap exists. In this case intrinsic charge transfer occurs between the GaSb and InAs layers, resulting in coexisting electron and hole populations.[9]

In this paper we study electron intersubband transitions within the InAs well, activated using magnetic fields applied parallel to the superlattice layers for a wide range of samples. This allows us to make an extensive study of the subband energies as a function of layer width. The parallel magnetic field induces a diamagnetic shift[10] of the subbands, as seen before in quantum-well structures, and also causes the electron and hole dispersion relations to shift relative to each other in k space.[11] The latter effect of the parallel field will thus decouple the bands causing further changes to the single-particle intersubband energies. The observed electron intersubband energies are compared with an eight-band self-consistent $\mathbf{k}\cdot\mathbf{p}$ model.

II. EXPERIMENT

The intersubband experiments were carried out on a series of 20, 40, and 80 period InAs/GaSb superlattices with various well and barrier thicknesses, grown by metal-organic vapor-phase epitaxy (MOVPE) on semi-insulating GaAs substrates.[12] To avoid dislocations and to accommodate the difference in lattice constant between the two binary materials, a $\sim$2-μm GaSb buffer layer was grown. Magnetotransport measurements carried out on the samples have confirmed the coexistence of holes and electrons; the results of two carrier fits to the Hall resistance are given in Table I for the samples studied.

Intersubband absorption is electric dipole in nature,[13] and therefore requires either an electric-field component of the light in the direction of the confining potential (the growth direction) or a mixing of the in and out of plane motion. This can be realized experimentally in a number of ways, well-reported elsewhere in the literature.[14] In this paper, we apply the magnetic field parallel to the superlattice layers, and illuminate the samples with either normal incidence or in a waveguide configuration, shown schematically in Fig. 1. In

TABLE I. The table shows the observed IST energies for the samples studied along with the layer thicknesses and electron and hole densities per layer. The superlattices consist of 20 periods of alternating InAs and GaSb layers unless stated otherwise. The layer thicknesses are determined by TEM results and growth rates.

	Thickness (Å)		Density (10^{11} cm^{-2})		
Sample	InAs	GaSb	Electron	Hole	Observed IST (meV)
OX2035 (40 wells)	110	90	1.5		109
OX2029 (40 wells)	110	100	1.3	1.1	106
OX1135	145	245	7.3	4.2	90
OX2058	220	180	6.9	6.85	64
OX1692	275	90	4.3	2.3	56
OX1137	280	190	7.2	4.8	60
OX2064 (80 wells)	280	270	7.3	7.2	62
OX1691	300	110	5.5	4.0	56
OX2006	310	200	7.6	7.1	57
OX1690	330	110	5.0	4.5	54
OX1296	405	85	8.2	5.2	50
OX1558	465	110	8.1	4.8	50
OX1546	465	110	7.2	4.6	50
OX2337	540	385	7.4	5.7	46

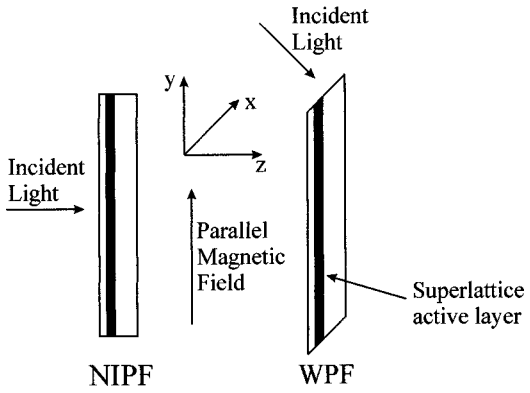

FIG. 1. A schematic showing the NIPF and WPF configurations. In both cases the field is orientated along the *y* axis, parallel to the superlattice layers.

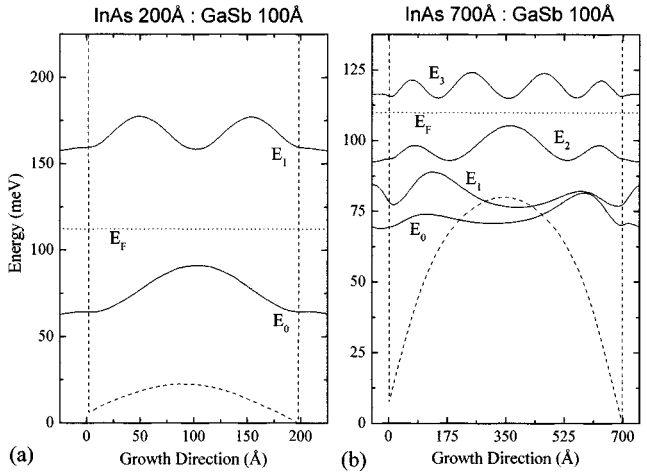

FIG. 2. The calculated electron wave functions for two structures with a constant GaSb barrier width of 100 Å and InAs values of 200 and 700 Å are shown in (a) and (b), respectively. The self-consistent well potential is shown as a dotted line. The creation of heterojunction bound states for structures with very wide wells is seen in the wider sample.

this orientation, quantization in the growth direction is determined by the superposition of the superlattice and magnetic potentials. Hybrid magnetoelectric subbands are formed, with the energies being field dependent. Throughout this paper we take the growth direction to be in the *z* axis with the magnetic field orientated parallel to the *y* axis. The parallel magnetic field causes the electrons to precess in the (*x*,*z*) plane and enables coupling of the electrons to the electric-field component of the light along the *x* axis. Thus, at finite parallel field the intersubband-transition (IST) selection rules for absorption are broken and normal-incidence intersubband absorption is made possible.

The majority of the samples were measured in the normal-incidence parallel field (NIPF) geometry where the light is incident normally onto the sample, in a direction parallel to the growth axis. For samples with narrower layers, where the field-induced absorption was measured at less than 8% using the NIPF, we use the multipass waveguide parallel field (WPF) geometry. In this setup the light is incident onto an optically polished edge, wedged at 45° with respect to the growth direction. The number of internal reflections that the light makes within the waveguide varied from sample to sample, but four double passes can be taken as a guide. The enhanced absorption of the multipass geometry enabled us to investigate samples with InAs well widths down to 100 Å. Unfortunately, the configuration is also found to completely absorb infrared radiation at energies below 68 meV, thus masking resonances at or below this energy [see inset Fig. 4(a)]. The far-infrared absorption is caused by the multipass geometry of the waveguide structures enhancing the tail of the GaAs reststrahlen and multiphonon absorption, and was found to be independent of both sample and applied magnetic field. Experiments performed on the same sample in the two different configurations confirmed that the intersubband resonance observed in each geometry is the same.

The experiments were carried out at a temperature of 2 K using a Bruker-Fourier transform spectrometer, with the samples mounted at the center of a 14 T superconducting magnet. The transmission of light through the samples was measured by a silicon bolometer mounted out of field center. As is usual for such a technique, the resulting spectra are a convolution of many parameters, and so the results presented here are ratioed against the zero-field spectra to show only the field-dependent absorption. This method allows us to measure field-induced changes in transmission of order 1–2% and proved far more satisfactory than the alternative method of ratioing against a sample of bulk GaSb, but unfortunately results in no knowledge of the nature of the absorption at zero field. We do not, therefore, seek to comment on the controversy surrounding normal-incidence intersubband absorption in antimonide structures, which has been thought to occur due to the highly anisotropic GaSb *L* valleys.[15]

III. RESULTS

To better understand the data presented below we shall first discuss the results of an eight-band self-consistent $\mathbf{k}\cdot\mathbf{p}$ model,[16] the details of which are beyond the scope of this paper. In the calculations we take the InAs (GaSb) band gap as 418 meV (810 meV), and a band offset of 150 meV between the GaSb valence band and InAs conduction band. The results show that the electron intersubband energy is primarily determined by the InAs well width and depends little on the width of the barrier. For the following discussion we have performed a number of calculations, varying the InAs width at a constant GaSb barrier width of 100 Å, to look at the energy variation of the electron subbands. Figure 2 shows the calculated wave functions for two different structures with InAs widths of 200 and 700 Å. The results for the thinner structure show the expected quantum-well picture, with only the ground-electron subband being occupied at this well width. On further increasing the well width the energy of the upper subbands falls as the heterostructure confinement is reduced, and for much wider wells (InAs width$>$350 Å) multiple subbands are occupied. For the widest structures, the conduction band potential splits the well into two halves with a heterojunction formed at each interface, as is shown in Fig. 2(b). The calculations show that the first two electron subbands (labeled E_0 and E_1) are confined by the heterojunctionlike potential at the interfaces, with the higher-excited subbands being bound by the whole well. In

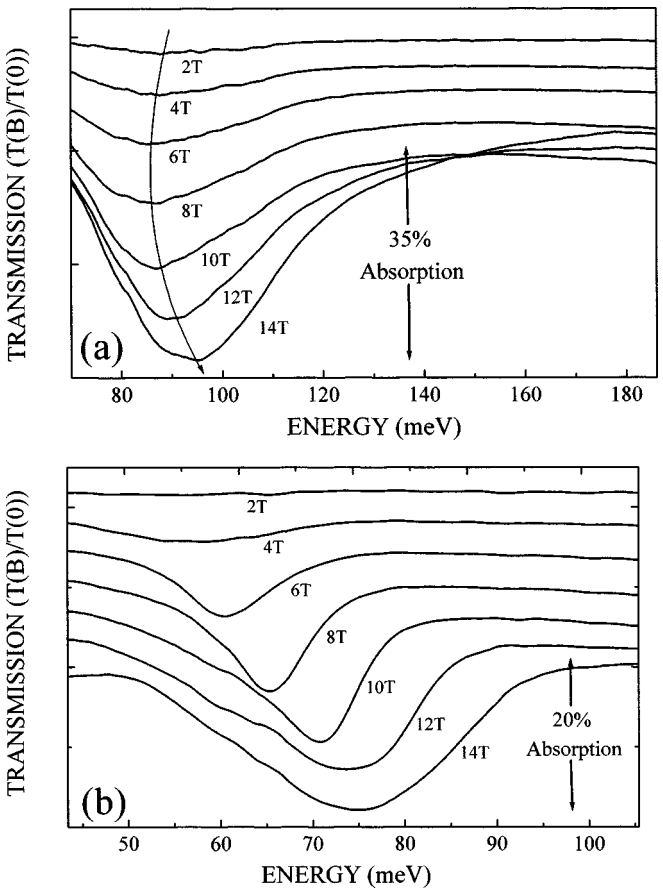

FIG. 3. Traces for the two thinner samples OX1135 (a) and OX1691 (b) measured in the WPF and NIPF configurations, respectively. The traces are ratioed against the zero-field value, and are shown for magnetic-field values 2, 4, 6, 8, 10, 12, and 14 T. In both cases the traces are offset for clarity. The arrow in (a) is to guide the eye.

this case we expect allowed intersubband transitions from the heterojunction confined subbands E_0 and E_1 to the well-bound subbands. Due to the small overlap between the two ground-heterojunction subbands, transitions between E_0 and E_1 are thought to be weak for such wide layers.

The experimental measurements have been performed on a number of samples with InAs well widths ranging from 100 to 540 Å. These show three general classes of behavior depending on well-width thickness, so for the purposes of this paper we will describe in detail three 20 period superlattice samples, which exhibit behavior characteristic for the given layer thickness. The field-induced absorptions for two samples with relatively thin InAs well widths are shown in Fig. 3. Conventional Hall and Shubinkov-de Haas measurements have shown that both these samples have only one occupied electron subband. The field-induced absorption strength of the thinnest sample OX1135, with a well width of 145, Å was found to be less than 8% in the NIPF configuration at full field. The sample was subsequently measured in the WPF configuration and exhibited an increased field-induced absorption of 38% at 14 T, and it is this data that is shown in Fig. 3(a). We observe a single resonance, which is strongly enhanced by the magnetic field, with an extrapolated zero-field energy of 90 meV. The magnetic-field dependence of the transition energy is small, due to the thin layers

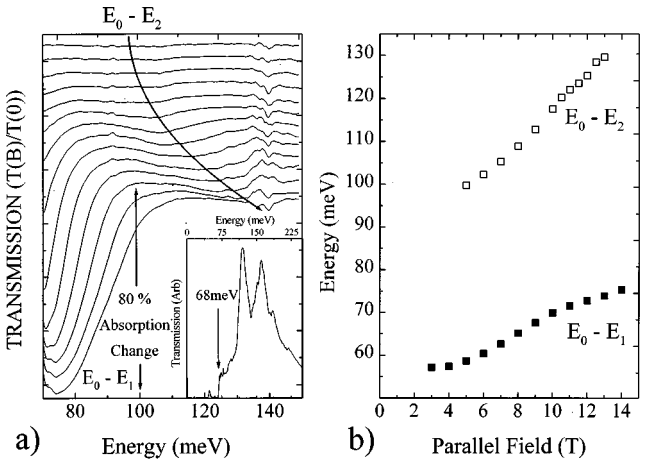

FIG. 4. (a) WPF measurements performed on sample OX1691 for magnetic-field values of 2, 4, 6, 8, 10, 12, and 14 T. The traces are ratioed against the zero-field trace and are offset for clarity. The inset shows the enhanced waveguide absorption of the GaAs restrahlen limiting transmission of the waveguide to energies above 68 meV. (b) The magnetic-field-induced diamagnetic shift of the two resonances is shown. The data points for the E_0-E_1 IST are deduced from the NIPF measurement.

causing strong electric confinement. This sample has a well width that is comparable to the multi-quantum-well structures studied by Gauer *et al.*,[17,18] and both the transition energy and absorption strength show a similar field dependence to this work. At the highest field the resonance shape becomes slightly distorted which may be evidence of a further splitting, analogous to the spin-flip transitions observed in the high carrier density InAs/AlSb samples of Gauer and co-workers.[17,18]

For sample OX1691, with an InAs well width of 300 Å, measurements were carried out in the NIPF configuration and are shown in Fig. 3(b). The increased InAs well width causes a decrease in the transition energy compared with OX1135 due to reduced carrier confinement; the zero-field IST being measured at 56 meV. The sample shows a greater field-induced absorption change of 18% (compared to 8% absorption change in the NIPF data for sample OX1135) and a stronger parallel field-induced diamagnetic shift, causing the transition energy to increase much more rapidly with increasing magnetic field. The dependence of both the absorption strength and transition energy on the InAs width and parallel field in these two samples leads us to believe that the absorption is due to the IST from the ground electron level (E_0) to the first excited level (E_1). Experiments have not been performed on the samples in the Brewster angle geometry to confirm the IST energies at zero parallel field; however, the similar and systematic behavior that we have observed in a wide range of samples has convinced us that the observed resonance is intersubband in nature.

Measurements have also been performed on OX1691 in the WPF configuration. In this case, we observe a field-activated resonance at the same energy as in the NIPF configuration, but with a much larger field-induced absorption change of 80% at 14 T. The waveguide geometry also reveals a second weaker resonance at higher energies, as shown in Fig. 4(a). The lower-energy resonance in the WPF configuration is masked below an energy of 68 meV due to

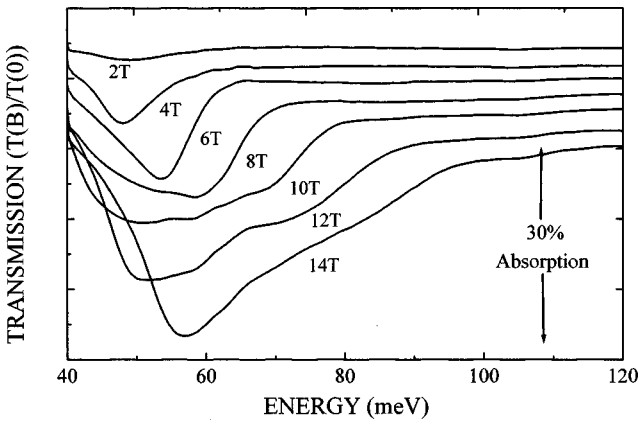

FIG. 5. The NIPF data for sample OX1558 is shown for parallel magnetic-field values of 2, 4, 6, 8, 10, 12, and 14 T. The traces are ratioed against the zero-field trace and offset for clarity. The two separate resonances, which dominate at high and low fields can be clearly seen.

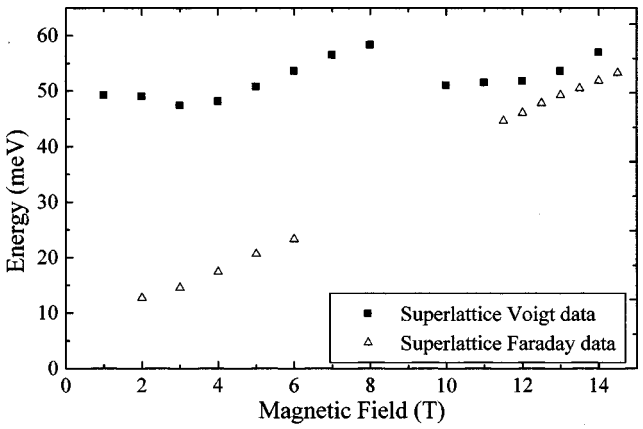

FIG. 6. Magnetic-field dependence of the two resonances observed in OX1558. The parallel-field data (squares) is compared with Faraday-configuration cyclotron resonance for the same sample (triangles).

the intrinsic absorption of the multipass waveguide geometry. Therefore, in the following discussion, the field dependence of the intersubband resonance is taken from the NIPF measurements shown in Fig. 3(b). The higher-energy resonance is found to be fast moving with field, diamagnetically shifted by 38 meV at 14 T compared with 18 meV for the E_0-E_1 transition, as shown in Fig. 4(b). The weaker resonance has a zero-field energy of 93 meV with a field-induced absorption change of 4% at 14 T compared with ~80% absorption change for the E_0-E_1 transition. The transition energy and strong diamagnetic shift leads us to believe that the second weaker resonance corresponds to the IST from E_0 to E_2. Although the E_0-E_2 transition breaks the selection rules for electric-dipole transitions, such that single photon absorption can only occur between subbands of opposite parity, the extremely weak absorption is observed due to subband asymmetry and mixing in the parallel-field orientation.

A second type of behavior is observed for superlattices with much wider wells where multiple electron bands are occupied. The samples were studied in the NIPF configuration and show a different magnetic-field dependence from the two thinner samples discussed above. We observe two main resonances that exchange intensity with increasing magnetic field, as shown in Fig. 5 for a typical sample OX1558, with an InAs width of 465 Å. At low fields a single field-activated resonance with an extrapolated zero-field energy of 50 meV is observed. The transition energy and absorption strength increase strongly with increasing magnetic field, the effect of small parallel fields being similar to the IST observed in the narrower layered samples. The transition energy at zero field is only slightly lower than in the medium thickness samples such as OX1691, but has a greater diamagnetic shift with applied magnetic field. The zero-field transition energy and the effects of parallel field on the absorption strength and transition energy again leads us to attribute this resonance to an IST. By this thickness, however, the theoretical calculations show that the conduction-band potential splits the well into two weakly coupled heterojunctions, with one at each interface. This effect has been previously observed experimentally using transport measurements in similar samples.[19] The observed IST is most likely to be a superposition of transitions from the heterojunction confined states to the well-bound subbands, although the measurements are only able to resolve a single transition. Further explanation of this transition and the effects of coupling between a number of different intersubband resonances will be discussed later.

At high fields, the IST is masked by a stronger lower-energy transition, which gains intensity with field. The resonance position of this lower-energy transition is found to be almost sample independent. For these samples the cyclotron radius (71 Å at 14 T) is considerably smaller than the well thickness, and we assign the change in behavior to a swapover to a three-dimensional cyclotron-resonance (CR) behavior at high fields. The transition between the two-dimensional IST behavior and the three-dimensional CR behavior is found to occur at a sample dependent field, such that for samples with wider wells the IST resonance switches to the lower-energy CR resonance at a lower magnetic field. The lower-energy resonance has been compared with cyclotron-resonance measurements performed in the Faraday geometry on this sample (electron mass of $0.028\,m_0$) as is shown in Fig. 6 (due to the complex asymmetric lineshapes only a single-resonance position has been plotted at the energy of minimum transmission). The observed high-field resonance in the NIPF configuration tends towards the Faraday geometry CR data at high fields. At higher fields than this we expect that the NIPF resonance behavior would tend more closely to the bulk InAs CR energy, as the heterostructure confinement potential becomes less important.

Evidence for the importance of the well width and the transition to well-bound orbits also comes from the magnetic-field dependence of the intersubband linewidth. This has been studied by fitting the resonances with a Lorentzian lineshape. The large absorption observed in the samples will induce a self-broadening of the linewidth, as is well known in the conventional CR model. This has been accounted for in the results shown below using a Drude formalism,[20] resulting in the real linewidth ΔB_r being given by:

$$\Delta B_r = \Delta B_{\mathrm{meas}} \left(\frac{T_B}{T_0} \right)^{1/2}, \tag{1}$$

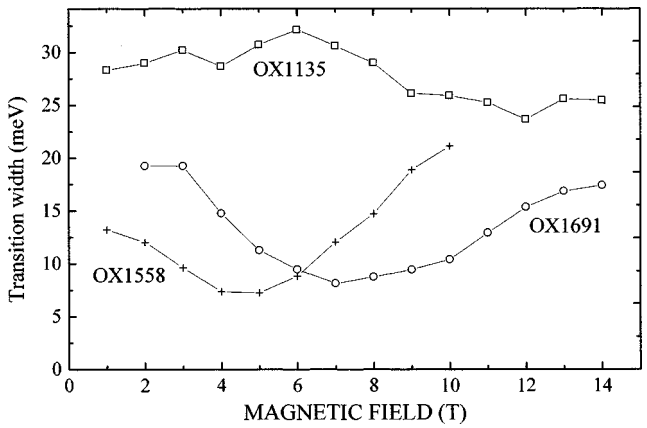

FIG. 7. The graph shows the variation of the intersubband linewidth for the three samples OX1135, OX1691, and OX1558. The data for the widest sample OX1558 is obscured at high-magnetic fields by the lower-energy resonance.

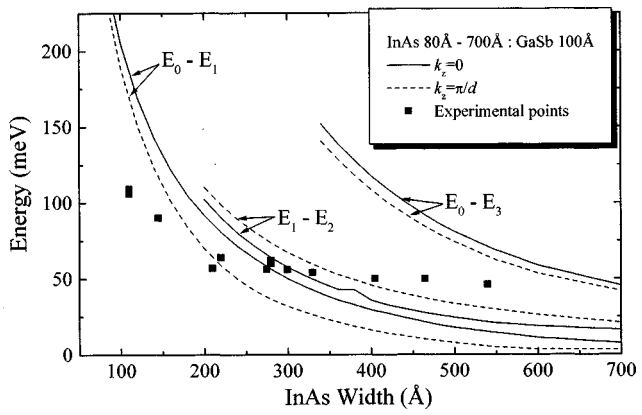

FIG. 8. The comparison between the experimentally determined zero-field intersubband energies (points) and the theoretical self-consistent $\mathbf{k}\cdot\mathbf{p}$ values. The theoretical values are given at $k_{\|}=0$, for both $k_z=0$ and $k_z=\pi/d$.

where ΔB_{meas} is the measured linewidth, and T_B and T_0 are the transmissions at finite field (B) and zero field, respectively, for the active component of the light, which in the case of NIPF is taken to be 50%. The absolute values should, however, be treated as only indicative due to the very asymmetric shape of the resonances in the widest-layer-width samples. The results are shown in Fig. 7 for the three samples studied above and show that a clear minimum in the linewidth is observed for the two wider-layered samples. The field at which this minimum occurs corresponds to $d \approx 4l_c$ where d is the well width and l_c the cyclotron length, with the data for the narrowest sample not reaching this condition. In the parallel-field geometry the relative size of the well compared to the cyclotron orbit will be important. At the position of minimum linewidth the electrons are easily able to execute cyclotron orbits within the well, and at fields a further factor of 2 higher the separate well-bound CR is observed. At lower fields than this the cyclotron orbit will be more complicated, either orbiting through both the well and barrier, or carrying out skipping orbits, as observed by Duffield.[21] The broadening at high fields could be explained by inhomogeneous broadening in which the variation in orbit center for the well-bound cyclotron orbits causes a spread of energies between the ISR and bulk CR values, as seen in the widest sample.

Further inspection of the lineshapes for both the thinner samples (OX1135 and OX1691) has revealed that these resonances are also somewhat asymmetric. The effect is seen most clearly for OX1691, which shows that for fields above 7 T the lineshape becomes asymmetric, with the higher-energy side being much sharper. Intersubband line broadening in AlGaAs/GaAs quantum wells has shown similar asymmetry of the lineshape and is attributed to the intrinsic conduction-band nonparabolicity.[22] In these experiments the lineshape will be influenced to a greater extent by the parallel magnetic-field-induced shift in k space,[10] which causes the carriers to be excited to a wider range of points in the k-space dispersion of the upper subband. The effect is far more pronounced in the wider of the two samples as expected, as this experiences a much greater diamagnetic shift.

The magnetic-field dependence of the IST also shows that a small negative diamagnetic shift is observed at low fields, the resonance position having decreased by 3–4 meV at 4 T. At fields higher than this the transition energy increases with field, and we observe the expected diamagnetically shifted IST. We speculate that this is evidence for electron-hole coupling causing small changes to the IST energies. In semimetallic structures band mixing between the electron and hole bands causes an anticrossing or small minigap to occur at finite k parallel.[23] The application of parallel field induces a relative shift in k space of the spatially separated carriers, which at high magnetic fields will cause a complete decoupling of the bands, thus destroying the minigap. The unexpected decrease in the IST energy at low fields is thought to originate from this parallel-field decoupling of the electron and hole dispersions. When the minigap is removed, the mean energy of the E_0 level rises due to the removal of the anticrossing effects, thus leading to the small decrease in the E_0-E_1 separation. Parallel-field magnetoresistance experiments performed on the same samples has shown strong evidence for the field-induced removal of the minigap,[24] with the largest effects observed at magnetic fields below 4 T where the electron and hole fermi surfaces are crossing each other.

IV. DISCUSSION

We now compare the experimentally determined intersubband energies at zero field with the IST energies obtained using the self-consistent model, as shown in Fig. 8. As discussed previously, the barrier width was found to have little effect on the electron intersubband energies, and thus has been fixed at 100 Å, which is typical for the measured samples. In the calculations the InAs well width ranges from 80 to 700 Å. The calculated results show that for the thinnest wells with thicknesses below 150 Å, the single-particle E_0-E_1 separation exceeds the measured values. Beyond this, for thicknesses of order 150–300 Å the calculated values of E_0-E_1 pass through the measured values. For the thicker wells, the wave functions begin to separate towards the two interfaces of the InAs layers, and we expect that the intersubband transitions will be from the heterojunction-bound subbands to the well-bound subbands. Due to coupling of the states in the two heterojunctions, E_0 and E_1 (see Fig. 2) will

form symmetric and antisymmetric states, and so transitions such as E_0-E_2 are not considered due to parity nonconservation. This transition was only observed as a very weak feature in the waveguide measurements performed on OX1691. The dominant intersubband transitions will be E_1-E_2 and E_0-E_3, the first excited subband E_1 becoming occupied at well widths greater than 300 Å. The experiment shows a continuous evolution of the transition from the E_0-E_1 IST to a resonance with an energy found to lie between the calculated values of the E_1-E_2 and E_0-E_3 IST's. The overall agreement with theory is reasonable, although the experimental variation of the transition energy with well width is much slower than the simple single-particle theory predicts. Two features need to be explained in detail. First, there is a discrepancy for very thin layers, and second, there is the fact that there is apparently a continuous evolution from the E_0-E_1 IST to a resonance with an energy between the calculated values of E_1-E_2 and E_0-E_3, with only a single resonance being observed at any one time. The single-particle model excludes two factors; first, dynamic screening of the electrons leads to a depolarization shift, which causes the resonance to be observed at higher energies; and second, the excitonic interaction between the excited electron and the hole it has left behind. In previous studies the effects are of a similar magnitude, with the former effect being somewhat stronger, and intersubband transition energies have been measured at energies slightly higher than the true intersubband separation. The reasons behind the discrepancy for the thinner samples cannot be attributed to depolarization or excitonic effects alone. Comparisons with measurements carried out on InAs/AlSb quantum wells are inconclusive, as it is found that there is also a large discrepancy between infrared absorption[25] and Raman[26] experiments performed on similar samples. The IR absorption experiments have shown a much-reduced intersubband transition energy ($\sim$70 meV) compared with the Raman experiments. In our present paper the intersubband transition energy for samples with comparable well widths shows good agreement with the IR results in the InAs/AlSb system. We do not offer an explanation for the discrepancy between the two different measurement techniques.

For the intermediate thickness samples where only a single resonance is observed, there are many previous examples of the coupling together of two resonances through both intersubband scattering and Coulomb interactions. This has been extensively treated theoretically,[27] mainly for the case of nondegenerate cyclotron-resonance transitions. Provided that the coupling is strong enough, then a single resonance is seen at the weighted mean energy. This would be entirely consistent with the observation of a continuous swap over from the E_0-E_1 IST to a resonance with an energy between E_1-E_2 and E_0-E_3 with layer thickness, due to the change in the wave functions. Using the Cooper-Chalker model the dimensionless interaction strength I of the coupling is given by

$$I=\frac{e^2l^2}{8\pi\varepsilon\varepsilon_0 a^3}\frac{1}{\hbar\delta\omega}, \tag{2}$$

where $\hbar\delta\omega$ is the energy separation of the two transitions, a is the interparticle spacing, and l is in the case of cyclotron resonance, the Larmor radius. The critical value for the interaction strength I is found to be 0.1, with the separate resonances being resolved for values less than this. In this present paper we write the Larmor radius in terms of the cyclotron frequency (ω_c) and replace $\hbar\omega_c$ with the energy of the observed transition. We find that the two transitions are separately resolved if the energy separation $\hbar\delta\omega$ is greater than 16 meV. The $\mathbf{k}\cdot\mathbf{p}$ calculations predict that the energy difference between the E_0-E_1 and E_1-E_2 IST's is very small over the entire range of InAs widths, and so such coupling between these resonances would be expected. For the samples with the widest wells the calculations suggest that separate E_1-E_2 and E_0-E_3 resonances might be observable. The energy separation (determined using $\mathbf{k}\cdot\mathbf{p}$) between these states is much larger than the minimum necessary estimated from the Cooper-Chalker model, but only a single well-defined resonance is seen in experiment. However, the spread of intersubband energies along k_z and $k_\parallel$ enhances the coupling causing a single resonance to be observed with a narrow linewidth much less than the spread of transition energies. A full calculation, which includes specifically the influence of the parallel field on the confinement potential and the k dispersion, can model the absorption features more precisely, and details will be published elsewhere.[28]

We will now compare the magnitude of the measured field-activated absorption change with previous studies and discuss its dependence on field and sample parameters. Intersubband studies have in the past concentrated on relatively narrow well-width samples, and so comparisons with the widest samples studied here are difficult to make. For the narrowest sample OX1135 with an InAs well width of 145 Å we observe in the NIPF geometry a field-induced absorption change of 8% at 14 T. This is similar to that seen in the 20 period 150 Å InAs/AlSb multiquantum-well sample studied by Gauer, who reported a 9% absorption at a parallel magnetic field of 13 T in a heavily doped sample ($n_e=2.5\times10^{12}\mathrm{cm}^{-2}$ per well). On increasing the well width to 300 Å (OX1691) the field-induced absorption change (at 14 T) is measured at 18%, and for the widest sample (OX1558) we observe an absorption change of 14% at a field of 6 T for the IST-type resonance; at higher fields than this the IST is masked by the stronger lower-energy resonance. The increase in absorption coefficient with well width is dominated by the dipole-matrix element, as the transition energy is only weakly dependent on the well width. The dipole-matrix element for the cyclotron-active polarization α_x is given by:[17]

$$\langle 1|H_{\mathrm{int}}|0\rangle=\frac{e}{m^*}\alpha_x eB\langle 1|z|0\rangle, \tag{3}$$

where the interaction Hamiltonian $H_{\mathrm{int}}=(e/m^*)\alpha\mathbf{P}$; $\mathbf{P}$ is the canonical momentum and α is the polarization vector. We find that the absorption coefficient depends qualitatively on the square of the well width over the range of samples studied. A more quantitative quadratic dependence of the absorption on parallel field is observed in all samples at low parallel-field values, and for the thinnest samples this continues up to high fields. For intermediate well widths ($200<l<350$ Å) the absorption strength increases with the square of the magnetic field for low-field values, but then moves to a more linear dependence at higher magnetic fields. The above

equation is derived in the approximation that the wave functions are solely determined by the heterostructure confinement, but for the case of wider wells there will be a considerable change at high fields where the perturbation approach breaks down. This will be considered in detail in a future publication.[28] The increase in absorption as a function of thickness is also consistent within the perturbation regime.

The experiments performed in the waveguide geometry have also shown large field-induced absorption of the IST with measurements on sample OX1691 giving an 80% increase in absorption at 14 T. In this geometry the unpolarized light is incident onto the surface of the wedged edge in the (y,z) plane, and thus has electric-field components in all three axial directions. The intrinsic intersubband absorption of the waveguide at zero field couples the electric-field component in the z direction (E_z), with the x and y components being inactive. Application of parallel magnetic field causes the x component of the electric field (E_x) to couple to the IST, which also becomes active. By ratioing the data against the zero-field trace we are only able to determine the field-induced change in total transmission and have no knowledge of the intrinsic zero-field coupling of the waveguide. We consider though that the large change in transmission observed in these samples cannot be attributed to absorption by the x component of the electric field only, and that the parallel field also induces some increased coupling of the intrinsic E_z component.

V. CONCLUSION

We have studied the infrared-absorption properties of semimetallic InAs/GaSb superlattices under the influence of parallel magnetic field, and at finite magnetic field have observed, normal-incidence excitation of the intersubband-dipole transition. Using a multipass waveguide geometry, we have been able to look at transitions in narrower samples in more detail, and also investigate transitions to higher subbands. The observed transition energies have been compared to eight-band $\mathbf{k}\cdot\mathbf{p}$ calculations and reasonable agreement is found for the samples with wider layers, although a disparity is found for the narrower samples.

ACKNOWLEDGMENTS

The research was financed by the Engineering Physical Research Council (U.K.) which we would like to thank for continued support. A.J.L.P. would also like to acknowledge financial support from The Technology Partnership (Cambridge, UK). Exchanges between UIA. Antwerp and Oxford are funded by the British Council.

[1] B. F. Levine, J. Appl. Phys. **74**, R1 (1993).
[2] N. P. Esiria, J. Appl. Spectrosc. **42**, 465 (1985).
[3] J. Bhan, Proc. SPIE **886**, 126 (1987).
[4] J. Faist, F. Capasso, C. Sirtori, D. L. Sivco, J. N. Baillargeon, A. L. Hutchinson, S.-N. G. Chu, and A. Y. Cho, Appl. Phys. Lett. **68**, 3680 (1996).
[5] R. Q. Yang and S. S. Pei, J. Appl. Phys. **79**, 8197 (1996).
[6] J. H. Roslund and T. G. Anderson, Superlattices Microstruct. **16**, 77 (1994).
[7] M. P. Mikhailova and A. N. Titkov, Semicond. Sci. Technol. **9**, 1279 (1994).
[8] A. Aardvark, G. G. Allogho, G. Bougnot, J. P. R. David, A. Giani, S. K. Haywood, G. Hill, P. C. Klipstein, F. Mansoor, N. J. Mason, R. J. Nicholas, F. Pascal-Delannoy, M. Pate, L. Ponnampalam, and P. J. Walker, Semicond. Sci. Technol. **8**, S380 (1993).
[9] D. M. Symons, M. Lakrimi, R. J. Warburton, R. J. Nicholas, N. J. Mason, P. J. Walker, M. I. Eremets, and G. Hill, Phys. Rev. B **49**, 16 614 (1994).
[10] W. Beinvogl, A. Kamgar, and J. F. Kock, Phys. Rev. B **14**, 4274 (1976).
[11] K. K. Choi, B. F. Levine, N. Jarosik, J. Walker, and R. Malik, Phys. Rev. B **38**, 12 362 (1988).
[12] G. R. Booker, P. C. Klipstein, M. Lakrimi, S. Lyapin, N. J. Mason, R. J. Nicholas, T.-Y. Seong, D. M. Symons, T. A. Vaughan, and P. J. Walker, J. Cryst. Growth **146**, 778 (1994).
[13] L. C. West and S. J. Eglash, Appl. Phys. Lett. **46**, 1156 (1985).
[14] M. Helm, Semicond. Sci. Technol. **10**, 557 (1995).
[15] L. A. Samoska, B. Brar, and H. Kroemer, Appl. Phys. Lett. **62**, 2539 (1993).
[16] T. A. Vaughan, Ph.D. thesis, Oxford University, 1995.
[17] C. Gauer, A. Wixforth, J. P. Kotthaus, G. Abstreiter, G. Weimann, and W. Schlapp, Europhys. Lett. **30**, 111 (1995).
[18] C. Gauer, A. Wixforth, J. P. Kotthaus, B. Brar, and H. Kroemer, Superlattices Microstruct. **19**, 241 (1996).
[19] R. W. Martin, M. Lakrimi, S. K. Haywood, R. J. Nicholas, N. J. Mason, and P. J. Walker, in *High Magnetic Fields in Semiconductor Physics III, Würzburg 1990*, edited by G. Landwehr, Springer Series in Solid-State Sciences Vol. 101 (Springer-Verlag, Berlin, 1992), p. 420.
[20] T. A. Kennedy, R. J. Wagner, B. D. McCombe, and J. J. Quinn, Solid State Commun. **18**, 275 (1976).
[21] T. Duffield, R. Bhat, M. Koza, F. Derosa, K. M. Rush, and S. J. Allen, Phys. Rev. Lett. **59**, 2693 (1987).
[22] M. Zaluzny, Phys. Rev. B **43**, 4511 (1991).
[23] M. Altarelli, Phys. Rev. B **28**, 842 (1983).
[24] M. Lakrimi, S. Khym, R. J. Nicholas, D. M. Symons, F. M. Peeters, N. J. Mason, and P. J. Walker, Phys. Rev. Lett. **79**, 3034 (1997).
[25] A. Simon, J. Scriba, C. Gauer, A. Wixworth, J. P. Kotthaus, C. R. Bolognesi, C. Nguyen, G. Tuttle, and H. Kroemer, Mater. Sci. Eng., B **21**, 201 (1993).
[26] J. Wagner, J. Schmitz, F. Fuchs, J. D. Ralston, and P. Koidl, Phys. Rev. B **51**, 9786 (1995).
[27] N. R. Cooper and J. T. Chalker, Phys. Rev. Lett. **72**, 2057 (1994).
[28] R. De Meester, F. M. Peeters, M. Lakrimi, R. J. Nicholas, A. J. L. Poulter, N. J. Mason, and P. J. Walker (unpublished).